This article was downloaded by: [Tomsk State University of Control Systems and Radio]
On: 18 February 2013, At: 13:11
Publisher: Taylor & Francis
Informa Ltd Registered in England and Wales Registered Number: 1072954 Registered office: Mortimer House, 37-41 Mortimer Street, London W1T 3JH, UK

Molecular Crystals and Liquid Crystals Science and Technology. Section A. Molecular Crystals and Liquid Crystals
Publication details, including instructions for authors and subscription information:
http://www.tandfonline.com/loi/gmcl19

Synthesis and Optical Properties of New Ferroelectric Liquid Crystals: (S)-(+)-Methyl-2-butyl-[4′-(4-n-alkoxybenzoyloxy)benzilidene]-4-aminobenzoate and (S) (+)-Methyl-2-butyl-[4′-(4-n-alkoxycinnamoyloxy)benzilidene]-4-aminobenzoate

Aloir Merlo [a] , Hugo Gallardo [a] , T. R. Taylor [b] & Teodosio Kroin [b]
[a] Departamento de Quimica, Universidade Federal de Santa, Catarina; 88.000, Florianópolis, SC, Brazil
[b] Departamento de Fisica, Universidade Federal de Santa, Catarina; 88.000, Florianópolis, SC, Brazil
Version of record first published: 24 Sep 2006.

To cite this article: Aloir Merlo , Hugo Gallardo , T. R. Taylor & Teodosio Kroin (1994): Synthesis and Optical Properties of New Ferroelectric Liquid Crystals: (S)-(+)-Methyl-2-butyl-[4′-(4-n-alkoxybenzoyloxy)benzilidene]-4-aminobenzoate and (S) (+)-Methyl-2-butyl-[4′-(4-n-alkoxycinnamoyloxy)benzilidene]-4-aminobenzoate, Molecular Crystals and Liquid Crystals Science and Technology. Section A. Molecular Crystals and Liquid Crystals, 250:1, 31-39

To link to this article: http://dx.doi.org/10.1080/10587259408028190

PLEASE SCROLL DOWN FOR ARTICLE

Full terms and conditions of use: http://www.tandfonline.com/page/terms-and-conditions

This article may be used for research, teaching, and private study purposes. Any substantial or systematic reproduction, redistribution, reselling, loan, sub-licensing, systematic supply, or distribution in any form to anyone is expressly forbidden.

The publisher does not give any warranty express or implied or make any representation that the contents will be complete or accurate or up to date. The accuracy of any instructions, formulae, and drug doses should be independently verified with primary sources. The publisher shall not be liable for any loss, actions, claims, proceedings, demand, or costs or damages whatsoever or howsoever caused arising directly or indirectly in connection with or arising out of the use of this material.

Downloaded by [Tomsk State University of Control Systems and Radio] at 13:11 18 February 2013

Mol. Cryst. Liq. Cryst., 1994, Vol. 250, pp. 31–39
Reprints available directly from the publisher
Photocopying permitted by license only
© 1994 Gordon and Breach Science Publishers S.A.
Printed in the United States of America

Downloaded by [Tomsk State University of Control Systems and Radio] at 13:11 18 February 2013

Synthesis and Optical Properties of New Ferroelectric Liquid Crystals: (S)-(+)-Methyl-2-butyl-[4′-(4-*n*-alkoxybenzoyloxy)benzilidene]-4-aminobenzoate and (S) (+)-Methyl-2-butyl-[4′-(4-*n*-alkoxycinnamoyloxy)benzilidene]-4-aminobenzoate

ALOIR MERLO and HUGO GALLARDO

Departamento de Química, Universidade Federal de Santa Catarina; 88.000 Florianópolis, SC, Brazil

and

T. R. TAYLOR and TEODOSIO KROIN

Departamento de Física, Universidade Federal de Santa Catarina; 88.000 Florianópolis, SC, Brazil

(Received May 10, 1993)

Four members of (S)-(+)-Methyl-2-butyl-[4′-(4-*n*-alkoxybenzoyloxy)benzilidene]-4-aminobenzoate (Series I) and four members of (S)-(+)-Methyl-2-butyl-[4′-(4-*n*-alkoxycinnamoyloxy)benzilidene]-4-aminobenzoate (Series II) were synthesized. Both series show cholesteric, smectic A and smectic C* phases. The phase transition behavior is described and measurements of the optical tilt angle and helix pitch in the smectic C* phase are presented.

Keywords: (S)-(+)-Methyl-2-butyl-[4′-4-n-alkoxybenzoyloxy)benzilidene]-4-aminobenzoates, S-(+)-Methyl-2-butyl-[4′-4-n-alkoxycinnamoyloxy)benzilidene]-4-aminobenzoates, ferroelectric liquid crystals, smectic C phases*

1. INTRODUCTION

The occurrence of spontaneous electric polarization in non orthogonal smectic phases consisting of chiral molecules and the electrooptical applications that result from this ferroelectricity have stimulated the synthesis and study of the physical properties of compounds containing one or more chiral centers.

The molecules of compounds which exhibit non orthogonal smectic phases gen-

Downloaded by [Tomsk State University of Control Systems and Radio] at 13:11 18 February 2013

erally consist of mixed aliphatic-aromatic organic systems (i.e. the absence of highly polar terminal groups). The central aromatic structure or core contains a number of polar groups. The core functional groups normally give a resultant lateral dipole across the long molecular axis which favors the formation of smectic phases. The alkyl/alkoxy terminal chains normally need 7 or more carbon atoms to show non orthogonal phases.[1] Molecules containing phenyl-carboxylates or phenyl-cinnamate groups in the core are promising candidates for development of ferroelectric phases. Molecules containing these groups generate compounds that have a tendency to exhibit smectic C phases over a considerable temperature range and frequently with the presence of smectic A phases. The presence of a smectic A phase above the smectic C is generally an advantage as this usually makes alignment of the smectic C phase easier.

In this paper we report on four members of (S)-(+)-Methyl-2-butyl-[4′-(4-*n*-alkoxybenzoyloxy)benzilidene]-4-aminobenzoate, series I and four members of series II, (S)-(+)-Methyl-2-butyl-[4′-(4-*n*-alkoxycinnamoyloxy)benzilidene]-4-aminobenzoate. The general structure of each series is shown below:

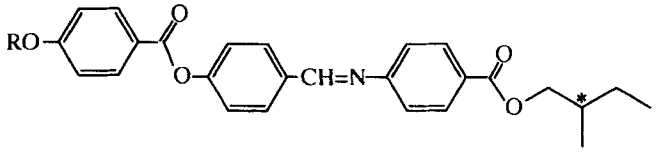

$R = C_n H_{2n+1}$

n = 5, 8, 10, 12

SERIE I

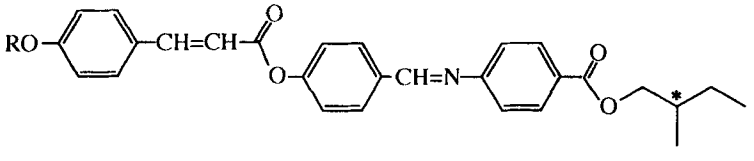

$R = C_n H_{2n+1}$

n = 7, 9, 12, 13

SERIE II

2. SYNTHESIS

The chiral starting material for the two series is (S)-(−)-2-Methyl-1-butanol, which is readily available in acceptable enantiomeric purity. The synthesis is carried out as outlined in Scheme 1. The homologous series were prepared via well-known

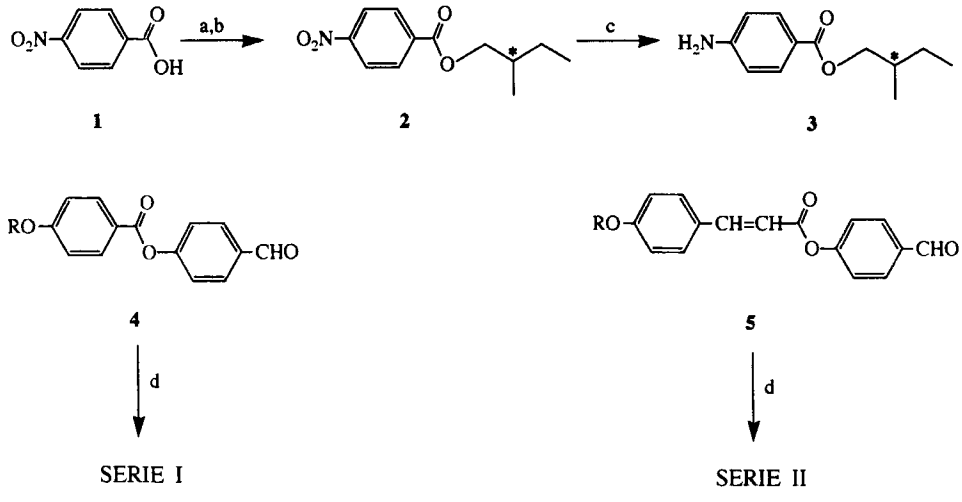

(a) $SOCl_2$; (b) (S)-(-)-2-Methyl-1-butanol, Py; (c) H_2, Pd/C, EtOH; (d) (S)-(+)-2-Methylbutyl-4-aminobenzoate (3).

SCHEME 1

synthetic processes, using ethyl-*p*-hydroxybenzoate, *p*-nitrobenzoic acid, malonic acid and *p*-hydroxybenzaldehyde as starting materials. (S)-(+)-4-amino(2-methylbutyl)benzoate (3) is a very useful reagent for preparing different compounds. This reagent when treated with the corresponding aldehyde undergoes a condensation reaction in high yield.

3. MESOPHASE IDENTIFICATION

The transition temperatures for all compounds were determined by optical microscopy using a Leitz Ortholux Polarizing Microscope in conjunction with a Mettler FP-52 heating stage. The transition temperatures were also determined from DSC measurements using a Perkin-Elmer DSC-2 excepting the Sm C*-Sm A transition where the transition enthalpy is vanishing small. The transition temperatures cited are for bulk samples. When the thickness of the sample is on the order of a few microns, as in the optical measurements in the next section, there are small variations in the Sm C*-Sm A transition temperature.

The phases were identified by observation of textures and convergent light observations. In all compounds, after the isotropic-cholesteric (I-Ch) transition there was a temperature interval of approximately two degrees with what we identify as a blue phase although measurements with the highest sensitivity range of the DSC did not show any blue phase transitions. As the temperature is lowered a cholesteric planar texture is observed in aligned samples with selective reflection in the visible spectrum. Racemic compounds showed typical nematic textures. The Sm A showed

Downloaded by [Tomsk State University of Control Systems and Radio] at 13:11 18 February 2013

a strong tendency to assume the homeotropic texture but the focal conic fan texture was also observed. Convergent light observations on the homeotropic texture gave a centered uniaxial positive cross. The texture of the Sm C* was "homeotropic"[2] if the preceding Sm A was homeotropic and broken fan (normally with black bands due to the helix) if the preceding Sm A showed the fan texture. Some measurements were made on the "homeotropic" Sm C* texture with an electric field applied parallel to the smectic layers to unwind the helix.[3] With an applied electric field parallel to the layers and in convergent light, at the Sm A-Sm C* transition the centered uniaxial cross of the Sm A becomes a biaxial cross and inclines rapidly, eventually saturating at an angle of 20 to 30 degrees. Originally we intended to use this method to measure the optical tilt angle but the optical field available with the Mettler hot stage is too small to permit precise measurement of large tilt angles.

Table I and Table II summarize the phase behavior as a function of temperature. The major difference between series II and series I is that almost all transition temperatures of series II are ten to twenty degrees higher than those of series I.

4. TILT ANGLE AND HELIX PITCH

For measurement of the Smectic C* tilt angle the compounds were sandwiched between two glass plates with ITO electrodes of 5 × 5 mm. The electrodes were first spin-coated using a polyvinyl alcohol solution (0.05 percent by weight) and baked at 125°C. The plates were then rubbed gently in one direction several times on a lint free cloth. The plates were mounted together with the rubbing directions antiparallel without spacers under uniform pressure and the sample cell filled by

TABLE I

Mesomorphic ranges for serie I

n	K		SmC*		SmA		Ch		I
5	•	126.0	•	(109.0)	•	176.6	•	202.7	•
8	•	95.6	•	133.9	•	180.8	•	192.2	•
10	•	83.5	•	139.0	•	195.0	•	199.5	•
12	•	76.2	•	140.5	•	177.8	•	178.7	•

TABLE II

Mesomorphic ranges for serie II

n	K		SmC*		SmA		Ch		I
7	•	82.0	•	152.3	•	204.6	•	224.6	•
9	•	57,9	•	164,8	•	205,0	•	216,3	•
12	•	67,0	•	165,4	•	196,5	•	198,5	•
13	•	68,5	•	166,0	•	198,8	•	200,5	•

Downloaded by [Tomsk State University of Control Systems and Radio] at 13:11 18 February 2013

capillary action in the cholesteric or isotropic phase. The cell thickness was estimated by compensation of the interference color of aligned samples using a quartz wedge with determination of the interference order of the wedge by observation of air bubbles. Assuming a maximum birefringence of 0.2 for the smectic phases, we calculated that the sample thickness was less than 4 μm.

Planar alignment of the liquid crystal was usually done by shearing the glass plates in the Sm A or Sm C* although at times it was possible to obtain planar alignment without shearing. We almost always obtained excellent alignment close to the Sm A-Sm C* transition but with decrease in temperature the alignment quality always deteriorated. At times it was possible to regain an excellent alignment by shearing again at lower temperatures.

The tilt angle was measured using the polarizing microscope and with crossed polarizers, a DC voltage of 15 V was applied to the cell and the microscope stage adjusted to give extinction. Then the polarity of the DC voltage was inverted and the stage adjusted to the new extinction position; the angle between the two extinctions positions is taken to be twice the tilt angle. Although the apparent quality of the alignment was always excellent it was relatively common to obtain tilt angles that were smaller than what we knew to be the true tilt angles. Presumably, this indicates that there existed, at times, a layer tilt (i.e., the chevron structure) which gives a measured tilt angle smaller than the true tilt angle.

Graphs of the tilt angle versus temperature are shown in Figures 1 and 2. The

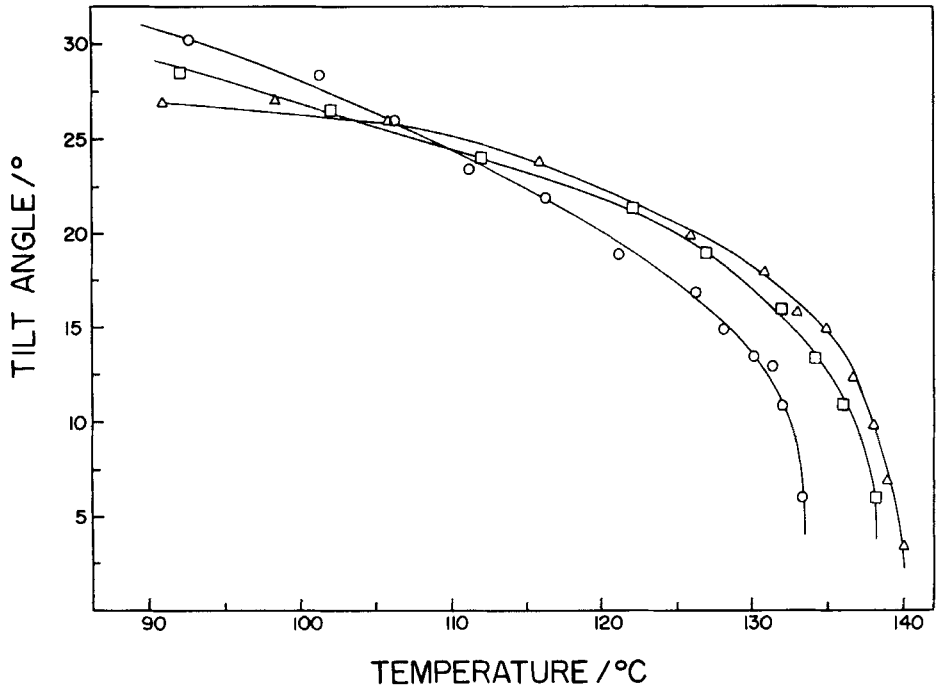

FIGURE 1 Smectic C* tilt angle as a function of the temperature for compounds of Series I. Symbols: open circle, $n = 8$; open square, $n = 10$; open triangle, $n = 12$.

Downloaded by [Tomsk State University of Control Systems and Radio] at 13:11 18 February 2013

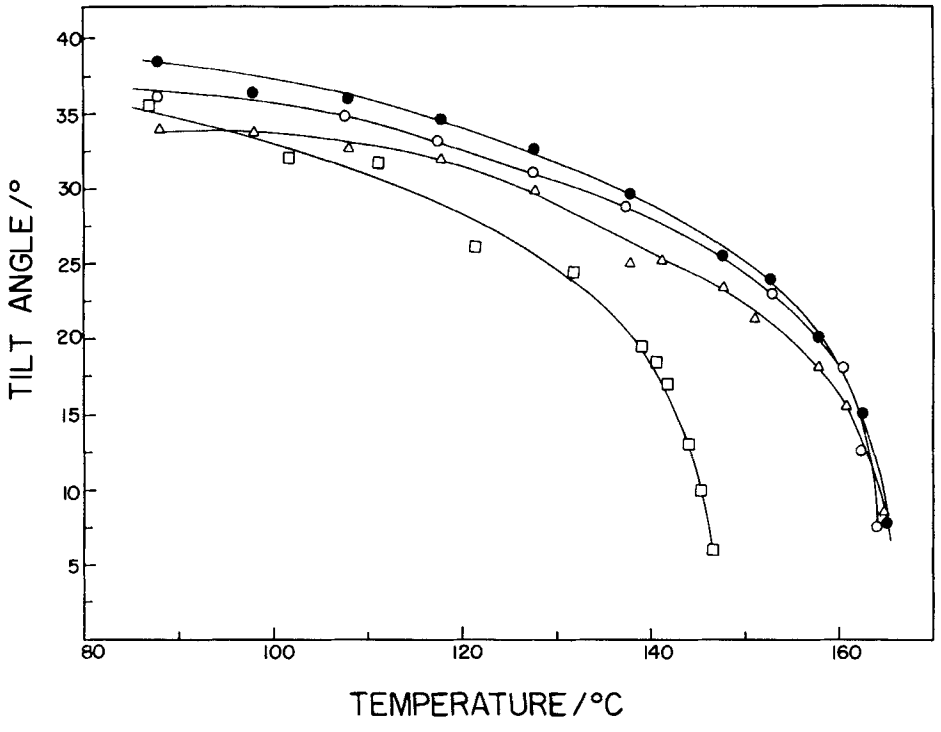

FIGURE 2 Smectic C* tilt angle as a function of the temperature for compounds of Series II. Symbols: open square, $n = 7$; filled circle, $n = 9$; open circle, $n = 12$; open triangle, $n = 13$.

compounds of series II have a saturation tilt angle on the order of 30 to 40 degrees and those of series I a saturation angle on the order of 25 to 30 degrees. The tilt angles reported are those that we think correspond to no layer tilt (i.e., maximum values of the measured tilt angle) and where the same angles were measured on two different samples. We did not observe the presence of optical bistability under an electric field in these compounds.

The Sm C* phase helical pitch was measured by the laser diffraction method. Alignment was obtained using the same method as in the tilt angle measurements; a sample thickness of 180 μm was obtained using mylar spacers. Some samples with a thickness of 340 μm were made to check the effect of wall anchoring on the measured pitch. The pitch measured with the two thicknesses was the same within experimental error and therefore we present results measured on 180 μm thick samples. All measurements were made on cooling. The quality of the diffraction pattern was always good until about 20 degrees below the Sm A-Sm C* transition. At lower temperatures the pattern progressively deteriorates as has been reported previously.[4]

Figures 3 and 4 show the variation of the pitch with temperature. Both series show similar behavior of the pitch; the pitch is on the order of 10 μm near the transition to the Sm A and at lower temperatures tends to a constant value of about 2 to 4 μm.

Downloaded by [Tomsk State University of Control Systems and Radio] at 13:11 18 February 2013

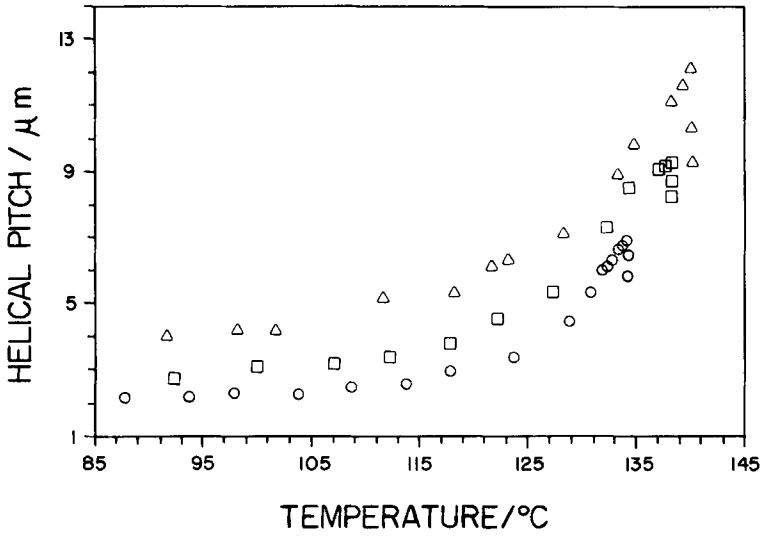

FIGURE 3 Smectic C* helix pitch as function of the temperature for compounds of Series I. Symbols: open circle, $n = 8$; open square, $n = 10$; open triangle, $n = 12$.

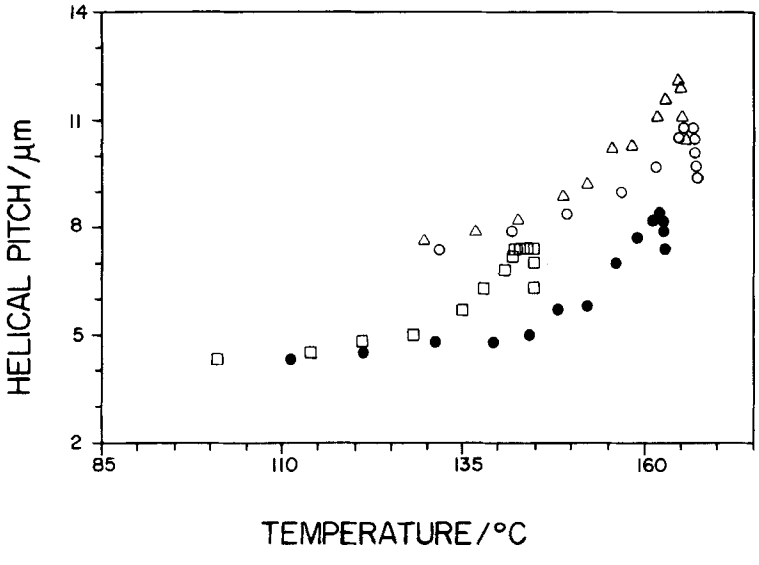

FIGURE 4 Smectic C* helix pitch as function of the temperature for compounds of Series II. Symbols: open square, $n = 7$; filled circle, $n = 9$; open circle, $n = 12$; open triangle, $n = 13$.

5. EXPERIMENTAL

The purity of the compounds was determined by thin layer chromatography (TLC) and elemental analysis (Tables III and IV). I.R. spectra were recorded for KBr discs with a Perkin-Elmer model 283 spectrometer, and ^{1}H NMR spectra were recorded at 60 MHz (Varian T-60).

Downloaded by [Tomsk State University of Control Systems and Radio] at 13:11 18 February 2013

TABLE III

Yields and elemental analyses of series I

n	Molecular Formula	Crude Yields %	Found (%) (Required) C	H	N
5	$C_{31}H_{35}NO_5$	85	74.9	7.1	2.7
			(74.3)	(6.9)	(2.8)
8	$C_{34}H_{41}NO_5$	80	74.9	7.3	2.5
			(75.1)	(7.5)	(2.6)
10	$C_{36}H_{45}NO_5$	83	75.3	7.8	2.4
			(75.6)	(7.8)	(2.4)
12	$C_{38}H_{49}NO_5$	81	76.8	8.5	2.4
			(76.1)	(8.2)	(2.3)

TABLE IV

Yields and elemental analyses of series II

n	Molecular Formula	Crude Yields %	Found (%) (Required) C	H	N
7	$C_{35}H_{41}NO_5$	72	76.1	7.3	2.3
			(75.8)	(7.4)	(2.5)
9	$C_{37}H_{45}NO_5$	75	76.8	7.9	2.3
			(76.2)	(7.7)	(2.4)
12	$C_{40}H_{51}NO_5$	80	76.7	8.0	2.3
			(76.8)	(8.2)	(2.2)
13	$C_{41}H_{53}NO_5$	82	77.0	8.2	2.3
			(76.9)	(8.3)	(2.2)

The 4-*n*-alkoxybenzoic acids were obtained from ethyl-*p*-hydroxy benzoate under standard Williamson esterification conditions. The corresponding acid chlorides were prepared by treatment of the acid with freshly distilled thionyl chloride.

The 4-(4′-*n*-alkoxybenzoyloxy)benzaldehydes were prepared by the methods of Reference 5.

(S)-(+)-4-amino(2-methylbutyl)benzoate (3) was prepared by methods described in the literature.[6,7] Data: $[\alpha]_D$ = 13.9° (C 3.9 g $CHCl_3$); m.p. 45–46°C. ^{1}H NMR ($CDCl_3$, TMS, 60 MHz): δ = 0.9 (m, 8H); 1.3 (m, 1H); 4.1 (d, 2H, J = 7 Hz); 4.3 (s, 2H); 6.7 (d, 2H, J = 8 Hz); 7.99 (d, 2H, J = 8 Hz).

The 4-(4′-*n*-alkoxycinnamoyloxy)benzaldehydes were prepared by the methods of Reference 8.

The Schiff Bases were prepared by standard methods and purified by chromatography on silica gel and recrystallized several times from ethanol or a mixture of hexane and benzene.

Physical data for series I, *n* = 10. ^{1}H NMR ($DCCl_3$, TMS, 60 MHz): δ = 0.89

Downloaded by [Tomsk State University of Control Systems and Radio] at 13:11 18 February 2013

(2t, 6H, J = 6.3 Hz, $-2CH_3$); 1.02 (d, 3H, J = 7.6 Hz, —CH_3); 1.13–2.13 (m, 19H, —$(CH_2—)_9$, —CH—); 4.13 (t, 2H, J = 7.0 Hz, —CH_2O—); 4.30 (d, 2H, J = 7.0 Hz, —$OC\underline{H}_2$); 7.17 (d, 2H, J = 8.0 Hz, Arom.); 7.30–8.43 (5d, 10H, J = 8.0 Hz, Arom.): 8.67 (s, 1H, —CH=N). I.R. (KBr): 2950, 2850, 1720, 1600, 1500, 1450, 1380, 1250, 1190, 1160, 1075, 720 cm^{-1}.

Physical data for series II, n = 13. ^1H NMR ($DCCl_3$, TMS, 60 MHz): δ = 0.90 (2t, 6H, J = 6.2 Hz, $-2CH_3$); 1.02 (d, 3H, J = 7.6 Hz, —CH_3); 1.12–1.87 (m, 25H, —$(CH_2)_{12}$, —CH—); 4.05 (t, 2H, J = 7.0 Hz, —OCH_2—); 4.20 (d, 2H, J = 7.0 Hz, —$OC\underline{H}_2$—CH—); 6.53 (d, H_A, J = 16.0 Hz, —$C\underline{H}_A$ = CH_x—); 7.73 (d, H_x, J = 16.0 Hz, —CH_A = $C\underline{H}_x$—); 7.04–7.70 (dd, 4H, J = 8.1 Hz, Arom.); 7.33–8.28 (dd, 4H, J = 8.0 Hz, Arom.); 7.34–8.35 (dd, 4H, J = 8.0 Hz, Arom.); 8.59 (s, H, —CH=N—). I.R. (KBr) 2950, 2850, 1720, 1600, 1550, 1450, 1380, 1250, 11190, 1160, 1075, 720 cm^{-1}.

Acknowledgment

This work was supported by the CNPq, FINEP/PADCT and FUNCITEC/SC.

References

1. J. W. Goodby, *Ferroelectrics*, **49**, 275 (1983).
2. G. W. Gray and J. W. G. Goodby, *Smectic Liquid Crystals—Textures and Structures*, Leonard Hill, Glassgow, 1984, p. 63.
3. E. Gorecka, A. D. L. Chandani, Y. Ouchi, H. Takezoe and A. Fukuda, *Jpn. J. Appl. Phys.*, **29**, 131 (1990).
4. K. Kondo, H. Takezoe, A. Fukuda and E. Kuze, *Jpn. J. Appl. Phys.*, **21**, 224 (1989).
5. H. Gallardo and F. C. Silva, *J. Chem. Soc. Perkin Trans. II*, 319 (1987).
6. B. D. Johnston and K. N. Slessor, *Can. J. Chem.*, **57**, 233 (1979).
7. A. A. Merlo and H. Gallardo, *Synth. Commun.*, **23**, 2159 (1993).
8. H. Gallardo, H. Muller, T. R. Taylor, M. Koerich and J. Moro, *Mol. Cryst. Liq. Cryst.*, **159**, 173 (1988).

Downloaded by [Tomsk State University of Control Systems and Radio] at 13:11 18 February 2013